Chapter 2

OPTIMAL SCHEDULING OF PEVS FOR CHARGING COST MINIMIZATION IN THE RE-CONFIGURABLE NETWORK CONSIDERING CVR

2.1 INTRODUCTION

The automobile industry is investing heavily in Plug-in Electric Vehicles (PEV) to taper CO_2 emissions and combustible fuel dependency. Electric Vehicles (EVs) not only have zero emissions but also have significantly lower noise levels. Apart from the environmental benefits, they could also deliver customer-centred benefits with lower operational costs if appropriately planned. Further, renewable energy sources such as photovoltaic and wind power can be used for charging these vehicles. The large-scale integration of PEVs adversely affects the load profile due to their arbitrary charging and discharging. This leads to more significant voltage deviations, higher line losses, and transformer overloading in a distribution system. Unregulated fast charging of PEVs further stresses the power system components and demands for capacity expansion, peak load shaving, and network re-configuration.

Despite all these challenges, PEVs having the capability of bi-directional power flow can also inject power to the grid while discharging, commonly referred to as the Vehicle-to-Grid (V2G) mode of operation. V2G deployment of the EVs can effectively reduce the peak demand and provide ancillary services. Charging schemes are proposed that allow EVs to operate in either V2G or Grid-to-Vehicle (G2V) mode, wherein aspects like system security and losses are assessed at different levels of EV penetration. Existing regulated charging schemes are able to improve distribution system performance to some

extent. Further research is required to develop an EV charging scheme that is more effective in flattening the load voltage profile and is more customer-centric as a result of charging cost reduction.

This research work provides optimal charging of PEVs in the existing distribution system with both V2G and G2V capabilities with the possibility of network re-configuration. PEVs charging under Conservation Voltage Reduction (CVR) to enhance distribution system performance is yet to be investigated. Therefore, an attempt has been made in this work to study distribution system performance under PEV charging carried out in a re-configured network with CVR deployment. It seems most of the works have not considered battery degradation cost in PEV charging cost optimization. This leads to over-estimation of customer benefits under the Time of Use (TOU)-based tariff structure. Therefore, the PEV charging cost optimization through the proposed scheme has considered battery degradation cost, too. The optimization has been performed under system operating constraints using linear programming.

2.2 PROBLEM DEFINITION AND FORMULATION

The proposed technique takes into account both the PEV owner's benefit and system conditions. Minimization of the formulated objective function is achieved under the set of constraints pertaining to PEVs as well as the distribution network.

The optimization methodology for developing the intelligent charging framework is based on the Linear Programming (LP) approach. The formulated problem is solved using the Interior-Point Method (IPM), i.e., Newton's method for equality constraints and the barrier method [89]. The method relies on solving a sequence of minimization problems with a linearized set of constraints. IPM allows one to solve a convex optimization

problem with inequality constraints as well. The minimization problem takes the general form as:

$$minimize\ f_0(x) \tag{2.1}$$

$$subject\ to\ f_i(x) \leq 0,\ i = 1,2 \ldots . m \tag{2.2}$$

$$Ax = b, \tag{2.3}$$

where, $f_0, \ldots . f_m : R^n \to R$ are convex and twice continuously differentiable. It is assumed that an optimal x^* exists, and the problem is strictly feasible. So, the dual optimal λ^* together with x^* satisfies Kuhn–Tucker (KKT) conditions.

$$Ax^* = b, \quad f_i(x^*) \leq 0,\ i = 1,2 \ldots . m \tag{2.4}$$

$$\lambda^* \geq 0, \tag{2.5}$$

$$\nabla f_0(x^*) + \sum_{i=1}^{m} \lambda_i^* \nabla f_i(x^*) + A^T v^* = 0 \tag{2.6}$$

$$\lambda_i^* f_i(x^*) = 0,\ i = 1,2 \ldots . m \tag{2.7}$$

The point $x^*(t)$ is m/t sub-optimal with feasible dual pair $\lambda_i^*(t), v^*(t)$. While incorporating inequality constraints using the barrier method, $x^*(t)$ is computed for a sequence of increasing values of time t till $t \geq m/\epsilon$. The algorithm for the barrier method is presented below.

Algorithm 1: *Barrier method*

Given: strictly feasible $x, t := t^0 > 0, \mu > 1, tolerance\ \epsilon > 0$.

do

1. *Centering step.*

Compute $x^\star(t)$ by minimizing $tf_0 + \varphi$, subject to $Ax = b$, starting at x.

2. *Update* x: $= x^\star(t)$.

---

3. *Stopping criterion* **end** if $m/t < \epsilon$.

4. *Increase* t, $t := \mu t$.

The formulated objective function for charging cost minimization, the combination of charging cost and battery degradation cost minimization, along with the set of constraints under which optimizations are performed, are presented below.

2.2.1 Charging cost of PEV

The operating cost of PEVs comprises the charging/discharging cost and battery degradation cost while neglecting the maintenance cost that does not fall in the scope of the work. The objective function for minimization of the charging cost incurred by the PEV owner is formulated with an assumption that the energy cost for charging and discharging is the same.

$$min \sum_{k=1}^{K} \sum_{n=1}^{N} ((X^{+})_{k}^{n} - (X^{-})_{k}^{n}) C_k \tag{2.8}$$

where, $(X^{+})_{k}^{n}$ is the charging rate and $(X^{-})_{k}^{n}$ is the discharging rate in kW, of n^{th} PEV in k^{th} time interval, C_k is the cost of energy in k^{th} time interval in \$/kWh, N is the number of PEVs that charge/discharge during a total number of K time intervals for an entire time duration of T.

2.2.2 Battery degradation cost in V2G scenario

The real power injection by the PEVs having bi-directional power transfer capability for providing grid support or reducing overall charging cost leads to the degradation of an EV battery. The life of the EV battery (the most commonly used Li-ion battery) is quantified in the number of charge/discharge cycles. The battery life in terms of energy throughput L_{ET}, can be calculated as:

$$L_{ET} = L_c \times E \times DOD \tag{2.9}$$

where L_{ET} is the energy throughput of the battery expressed in kWh, L_c is the charge/discharge cycle life of the battery, E is the energy stored in the battery, and DOD is the depth of discharge of the battery at specified L_c .

The battery degradation cost c_d, due to extra cycling is calculated as:

$$c_d = \frac{c_{bat}}{L_{ET}} \tag{2.10}$$

where, c_{bat} is the capital cost of the battery.

For example, the usable battery capacity of the EVs considered in this work is 27kWh, 2000 cycle life at 80% DOD, and the cost of battery per kWh is \$100. $L_{ET} = 2000 \times 27 \times 0.8 = 43{,}200$, and hence, the battery degradation cost is $c_d = \left(\frac{27\times100}{43200}\right) = 0.0625\$/kWh$.

The objective function for minimization of the battery degradation cost can be formulated as follows:

$$min \sum_{k=1}^{K} \sum_{n=1}^{N} (X^-)_k^n \, c_d^n \tag{2.11}$$

where, c_d^n is the battery degradation cost of n^{th} PEV.

To recapitulate, the objective function for minimization of the operating cost is expressed as follows:

$$min \sum_{k=1}^{K} \sum_{n=1}^{N} [(\,(X^+)_k^n - (X^-)_k^n)\, C_k + (X^-)_k^n c_d^n] \tag{2.12}$$

2.2.3 Constraints for PEV battery

The PEV charger having bi-directional power flow capability has limitations over its charging/discharging rate. For each PEV, this limitation is imposed as follows:

$$0 \leq \, (X^+)_k^n \leq (X^+)_{max}^n \,, \; k \in (T_a, T_d) \tag{2.13}$$

where, T_a is the arrival time of PEV and T_d is the indicated departure time of PEV.

$$0 \leq (X^-)_k^n \leq (X^-)_{max}^n \tag{2.14}$$

where, $(X^+)_{max}^n$ is the maximum charging rate and $(X^-)_{max}^n$ is the maximum discharging rate of n^{th} PEV.

Furthermore, a restriction on the State of Charge (SOC) value is imposed to avoid overcharging the PEV battery in order to preserve the battery lifecycles while charging the PEV to the desired SOC value by the departure time indicated by the PEV owner. The constraints on the SOC value are represented as:

$$SOC_{min}^n \leq SOC^n \leq SOC_{max}^n, \qquad \forall n = \{1,2,\dots,N\} \tag{2.15}$$

where, SOC^n is the state of charge of the battery, SOC_{min}^n is the minimum allowable SOC of the battery and SOC_{max}^n is the maximum allowable SOC of the battery of n^{th} PEV.

$$SOC_d^n = \left[SOC_i^n + \sum_{k=T_a}^{T_d} \frac{\left(\eta_{charging}^n (X^+)_k^n - \frac{(X^-)_k^n}{\eta_{discharging}^n} \right)}{E^n} \right], \forall n = \{1,2,\dots,N\} \tag{2.16}$$

where, SOC_d^n is the indicated SOC of n^{th} PEV as desired by the PEV owner, SOC_i^n is the initial SOC of the battery of n^{th} PEV at the time of plug-in, $\eta_{charging}^n$ is the charging efficiency, $\eta_{discharging}^n$ is discharging efficiency of the n^{th} PEV charger, and E^n represents stored energy in the battery of the n^{th} PEV. SOC_d^n given by equation (2.16) is to be multiplied by 100 to express it in percentage.

2.2.4 System constraints

In this work, a low voltage distribution system is considered with voltage V_t^i, at i^{th} bus at time instant, t. This voltage is restricted within a permissible tolerance of $\pm 10\%$.

$$V_{min}^i \leq V_t^i \leq V_{max}^i, \forall t = \{1,2,\dots,T\}, \forall i = \{1,2,\dots,I\} \tag{2.17}$$

where, V_t^i is the voltage at i^{th} bus in volts at time instant t, V_{min}^i is the minimum voltage limit at i^{th} bus, V_{max}^i is the maximum voltage limit at i^{th} bus, and I represents the total number of buses present in the system. Here, t is the time horizon variable covering the entire length of the day, i.e., 24h with a sampling of 30 mins.

2.3 CHARGING TARIFF FRAMEWORK

The literature has identified that a significant amount of EV charging is priced as residential entities. However, the energy tariffs for residential customers are heavily subsidized and are significantly low. Traditional energy tariff structure does not consider the real-time energy demand-supply gap, i.e., it offers flat or block rates. Therefore, customers receive no incentives for adjusting their power consumption following the market scenario.

Depending upon the power injected by the PEV charger into the battery, the PEV charging is categorized into three levels (i.e., A.C. Levels 1, 2, and 3). However, the current research considers Level 1 (3kW) residential charging since the tariff is minimum for residential customers. Level-2, fast PEV home charger consumption can go up to 19.2 kW with a typical of 7 kW, which exceeds the total demand of a typical household, and hence, it becomes obligatory to shift this load to the off-peak period. PEV charging load can be shifted away from peak hours by providing incentives to the customers in the TOU pricing structure. In a time-based pricing structure, the price for the power delivered is not fixed but depends upon the time block in which it is rendered. The energy price, the number of tiers, and block duration are fixed in advance from the historical load profiles. The most common and widely adopted dynamic pricing scheme is TOU pricing**.** In the TOU-based price scheme, pricing for energy consumption is fixed on hourly basis, and hence, they are known to the consumer in advance. This enables the consumer to receive

incentives by shifting the load to the off-peak period in which the electricity price is low. While using the TOU-based pricing model, EV owners can modify their charging schedule to reduce the charging cost and flatten the load profile.

We have considered the price per kWh of energy consumed in the off-peak load period, i.e.,$c_{off-peak} = 0.092\ \$/kWh$ [90]. While in the peak-load hours, the price, c_{peak} is calculated as:

$$c_{peak} = c_{off-peak} + c_{load\ threshold} \tag{2.18}$$

where, $c_{load\ threshold}$ is the penalty imposed on consumers to discourage over-loading. The measured power by the meter of the consumer is summed over the metered period T_s (30mins in our case). The kWh consumption so obtained for the metered period T_s is multiplied by the price per kWh ($c_{off-peak}$ or c_{peak} depending upon whether T_s corresponds to an off-peak period or peak period) to calculate the total charging cost of PEVs in the period T_s. The tariff structure considered in this work for 24 h duration is shown in Fig. 2.1. The time period considered in this work corresponds to 1:30 PM of one day to 1:30 PM of next day.

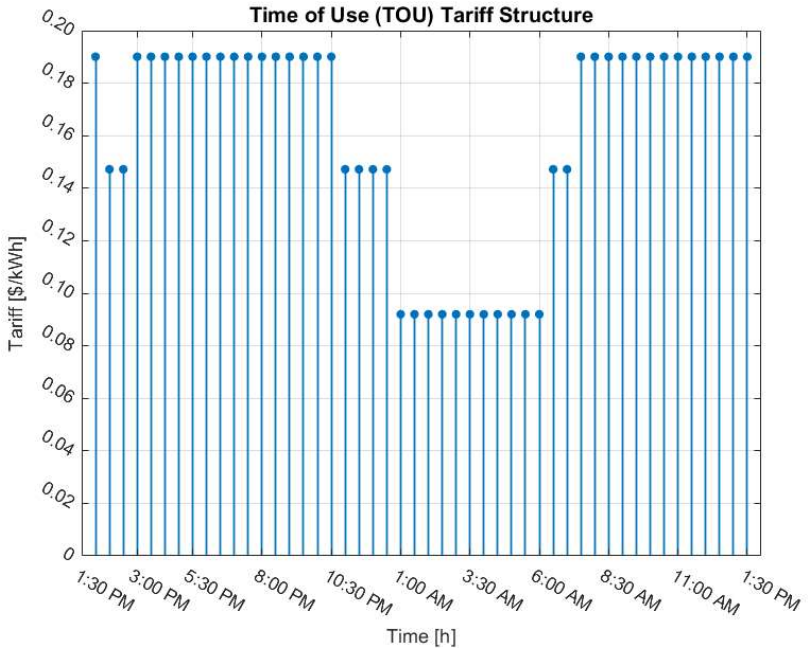

Fig. 2.1 Time of use (TOU) based electricity pricing.

2.4 GRAPHICAL APPROACH FOR NETWORK RE-CONFIGURATION

When dealing with distribution network re-configuration problems, the random initial populations generated by meta-heuristic methods create plenty of network topology. Some of these not only isolate system load buses but also tamper with the radiality of the network. Using graph theory combined with Fundamental Loops (FLs) ensures the removal of these unwanted network topologies by discarding infeasible switches during the network re-configuration process. In a Radial Distribution System (RDS), closing a normally opened set of switches creates an equal number of FLs as the number of tie switches. The test system considered in this work is a 33-bus distribution system, as shown in Fig. 2.2. In this test system, there are 32 normally closed branches and 5 normally opened tie-switches. The FLs are formed by closing the normally opened tie-switches s33, s34, s35, s36, and s37, as shown in Fig. 2.2. The elements of each FL can be obtained by selecting the tie-switches and closed branches associated with each fundamental loop. The graphical method representation of RDS is used to create the incidence matrix [C] of size $b \times nb$ where b and nb represent the number of buses and the number of branches, respectively, present in the system. The matrix [C] is formed using the elements C_{ij} as given by the expression:

$$C_{ij} = \begin{cases} 1, \ if\ branch\ i\ is\ away\ from\ j^{th}\ node \\ -1, \ if\ branch\ i\ is\ incident\ towards\ j^{th}\ node \\ 0, \ otherwise \end{cases} \tag{2.19}$$

To find the elements of 1st FL, an open tie-switch is closed, and the corresponding incidence matrix[C] is generated. By adding the absolute values of every element of each column of matrix [C], the columns with a sum with an absolute value equal to unity are marked, and rows corresponding to the marked column are eliminated. The step is

repeatedly exercised until the sum result is no more equal to 1. The resulting non-zero rows represent the elements of FL under analysis. Similarly, elements of all other FLs are obtained by closing the remaining tie-switches one at a time and following the same process followed for forming the first FL. In the binary coding system, a total of $2^{36} = 68719476736$ (31 branches and 5 tie-switches, open=0, close=1) combinations have to be checked (switch number s1 always remains closed as the opening will isolate all connected load in the system from the primary substation bus). As evident from Table 2.1, the creation of the FL ensures a total of $10 \times 7 \times 7 \times 16 \times 11 = 86240$ combinations, i.e., 10 switch positions in FL1, 7 switch positions in FL2, 7 switch positions in FL3, 16 switch positions in FL4 and 11 switch positions in FL5, thus substantially reducing the search space. During the re-configuration process, isolation of any load bus must be avoided while maintaining the network radiality. At least one switch must be selected from each FL of Table 2.1 as a re-configuration variable.

A graphical approach, spanning tree, is employed to ensure the distribution network radiality after switch selection without any load bus disconnected by opening these tie switches with all other switches closed. MATLAB logical condition $'graphisspantree\ (A)'$ is deployed for ensuring the network radiality while connection of all load buses is ensured using the length of Depth-First Searched (DFS) command $nbus_{traversed} = length(graphtraverse(A))$ with an open set of switches, where $matrix\ (A)$ is an undirected graph matrix, and DFS is depth-first search command to check the order of buses connected in the network. The step-wise algorithm to obtain the FLs while ensuring the system radiality is as follows:

Algorithm 2: Fundamental Loop formation algorithm

1: Generate incidence matrix C (branch-by-bus) using (2.20) of the network with all tie lines opened.

2: **procedure**

3: **while** $n \leq nb$ **do**

4: To generate the first FL, close the first tie-switch, and get the sum of absolute values of each element in each column of matrix C. Locate the column with a sum equal to 1, and remove the row corresponding to this column until the absolute sum of the element corresponding to each column becomes 0. Store the remaining branches in matrix C, representing the first FL.

5: **end while**

6: Choose one element from each FL representing switches to be opened to re-configure the network. Create adjacency matrix A with all the switches (i.e., tie switches) connected, except the chosen switches.

7: **if** $graphisspantree\ (A)' == 1$

8: Ensure the connection of all load buses using MATLAB function $length(graphtraverse(A))'$ equal to the total number of buses.

9: **else goto 6**

10: Calculate the objective function with the feasible set of re-configurable switches chosen.

11: **end procedure**

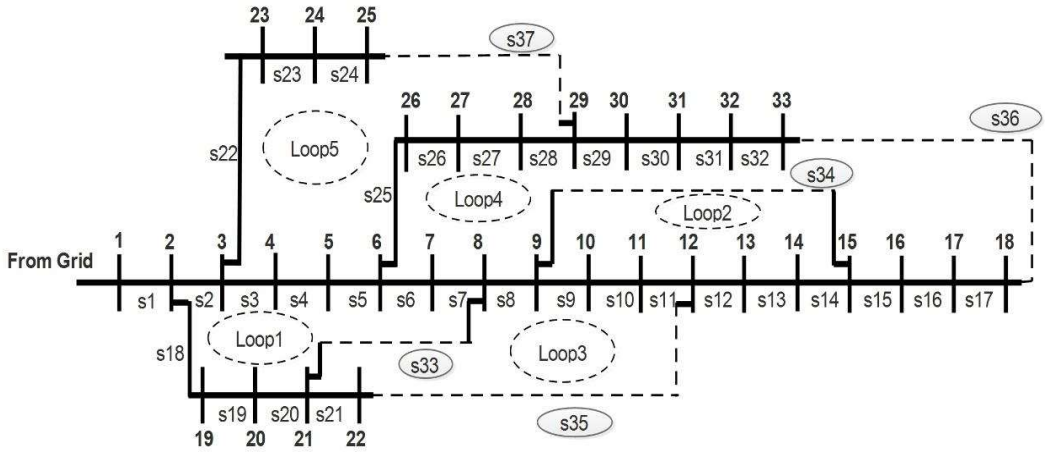

Fig. 2.2 Schematic of the IEEE 33-bus distribution system.

Table 2.1 Fundamental loops of the modified IEEE 33-bus system.

Switch Position	Fundamental Loops				
	FL1	FL2	FL3	FL4	FL5
1	s2	s9	s8	s25	s22
2	s3	s10	s9	s26	s23
3	s4	s11	s10	s27	s24
4	s5	s12	s11	s28	s37
5	s6	s13	s35	s29	s28
6	s7	s14	s21	s30	s27
7	s33	s34	s33	s31	s25
8	s20	0	0	s32	s26
9	s19	0	0	s36	s5
10	s18	0	0	s17	s4
11	0	0	0	s16	s3
12	0	0	0	s15	0
13	0	0	0	s34	0
14	0	0	0	s8	0
15	0	0	0	s7	0
16	0	0	0	s6	0

2.5 CONSERVATION VOLTAGE REDUCTION

Conservation Voltage Reduction (CVR) aims to reduce the power consumed by the electric load (constant impedance load) by lowering the operating voltage. The standard voltage range of secondary winding of the distribution transformer is 230 V ±10%, which translates into a permissible range of 207-253 V. CVR exploits this acceptable voltage range by operating the system near to lower limits for energy-saving without impacting the life of consumer appliances [91]. The efficacy of the CVR method can be quantified by a $CVR_{factor,i}$, for constant impedance load connected at bus i, which is defined as the ratio of the percent reduction in energy, $\Delta E_i\%$ consumed by constant impedance load at bus i to the percent reduction in voltage at bus i, $\Delta V_i\%$ as:

$$CVR_{factor,i} = \frac{\Delta E_i\%}{\Delta V_i\%} \tag{2.20}$$

$$\Delta E_i\% = \frac{E_{CVR\ off,i} - E_{CVR\ on,i}}{E_{CVR\ off,i}} \times 100 \tag{2.21}$$

$$\Delta V_i\% = \frac{V_{CVR\ off,i} - V_{CVR\ on,i}}{V_{CVR\ off,i}} \times 100 \tag{2.22}$$

where, $E_{CVR\ off,i}$ is the energy consumed by the constant impedance load at bus i without CVR, $V_{CVR\ off,i}$ is the voltage at bus i without CVR, $E_{CVR\ on,i}$ is the energy consumed by the constant impedance loads with CVR and $V_{CVR\ on,i}$ is the bus i voltage in the presence of CVR.

It is commented by the opponents of CVR that most loads are of constant power type. However, field validations have revealed that no load is purely a constant power, neither constant current nor a constant impedance type. Each electrical equipment having different characteristics can be modelled using ZIP coefficients.

The ZIP model in quadratic form can be expressed as:

$$P_i = P_{0i}\left[Z_{pi}\left(\frac{V_i}{V_{0i}}\right)^2 + I_{pi}\left(\frac{V_i}{V_{0i}}\right) + P_{pi}\right] \tag{2.23}$$

where, P_i is the power consumed by the loads at bus i, V_i is the voltage magnitude at bus i, V_{0i} is the rated voltage at bus i, Z_{pi} is the coefficient of the constant impedance component of load at bus i, I_{pi} is the coefficient of the constant current component of load at bus i and P_{pi} is the coefficient of the constant power component of load at bus i.

These coefficients can be obtained by the curve fitting based on the data obtained by performing experiments on a different class of electrical equipments.

2.6 CASE STUDY

The efficacy of the proposed PEVs scheduling scheme in TOU based tariff environment is presented in this section. PEV owners can exploit the TOU tariff structure by

discharging into the grid during peak and re-charging during off-peak price hours. Further, the proposed scheme is deployed on the re-configured test system for achieving higher cost benefits. The scheme is also tested in the presence of CVR.

Three different case scenarios are simulated on a down-scaled 33-bus active distribution test system for analysis. The nodes having PEV connections have been marked by a "dot," as shown in Fig. 2.3. The Distributed Energy Resources (DERs), wind and solar, are connected at nodes 18 and 33, respectively, with a penetration level of 15% each. The power generated by the DERs is shown in Fig. 2.4.

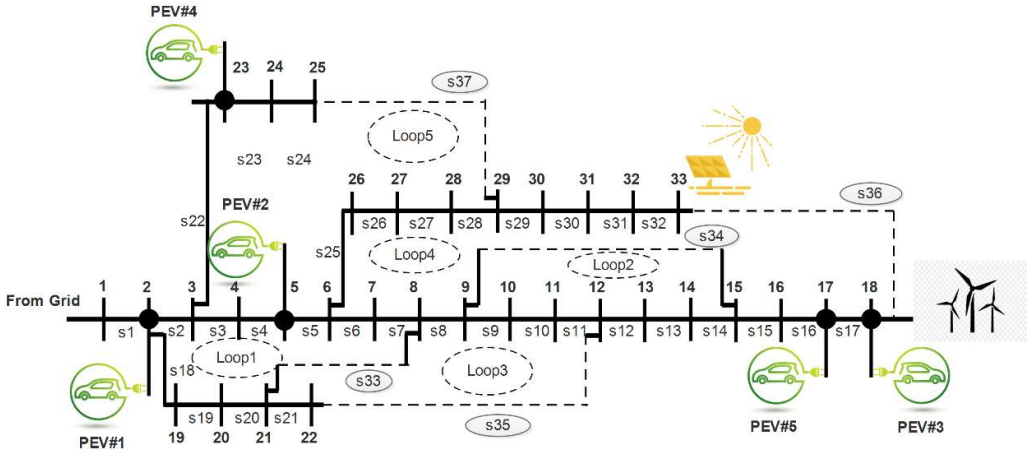

Fig. 2.3 Single line diagram of the test system.

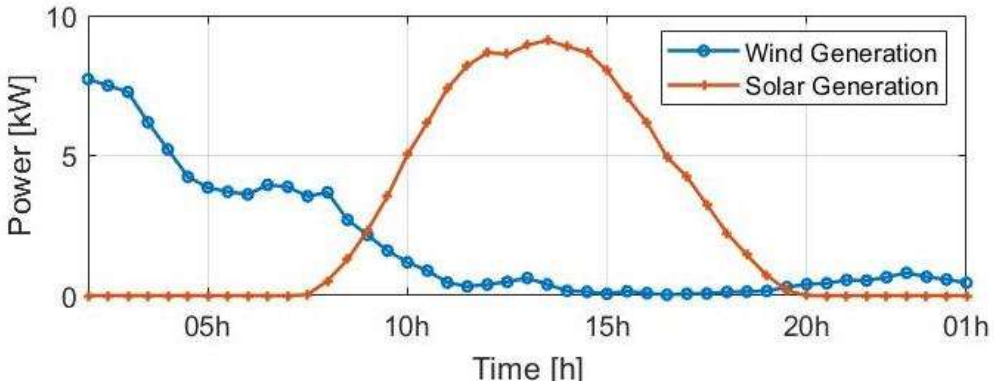

Fig. 2.4 Power generated by the DERs with a 15% penetration level.

2.6.1 Base case

The distribution system shown in Fig. 2.3 is fed by an 11/0.416 kV, 200 kVA distribution transformer. The voltage imposed on the nodes of the system is obtained using the backward/forward sweep-based optimal load flow method [92]. The voltage distribution of the system is shown in the form of a box plot in Fig. 2.5, wherein the central mark represents the median, the top and bottom edges of the box indicate the 75th and 25th percentile, and the marks out of the box on top and bottom edges represent maximum and minimum values. The outlier data points are shown by '+'.

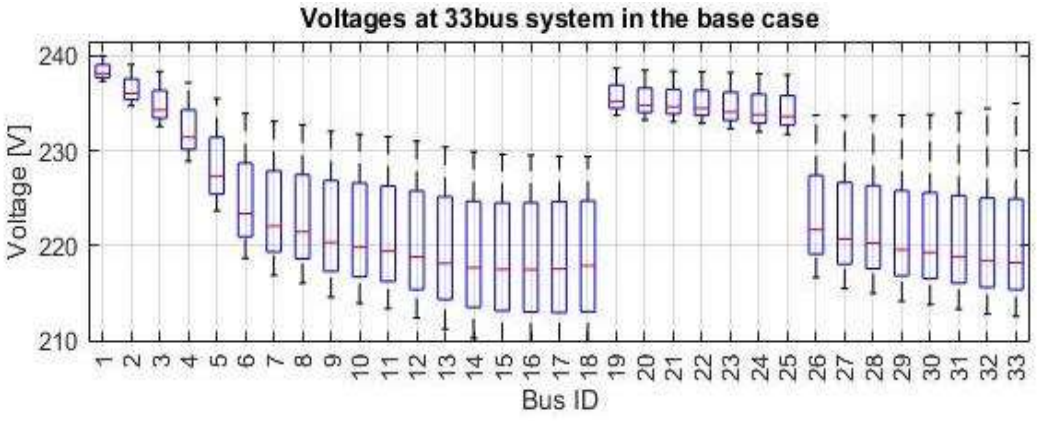

Fig. 2.5 Voltage distribution in the system without PEVs.

In this work, the maximum charging rate $(X^{+})_{max}^{n}$ for all the PEVs is considered to be 3kW and the maximum discharging rate $(X^{-})_{max}^{n}$ for all the PEVs is considered to be -3kW. Further, the minimum SOC level for all the PEVs, SOC_{min}^{n} is considered to be 0% and the maximum SOC level for all the PEVs, SOC_{max}^{n} is considered to be 100% with a total battery capacity of 30kWh (usable battery capacity of 27kWh). In the TOU-based tariff environment, the PEV owners have the opportunity of profit-making from the entire charging schedule. The PEVs with sufficient initial SOC discharge into the grid during peak price hours, respecting all the system constraints. The voltage profile of the system in the presence of PEVs is shown in Fig. 2.6, while the entire load on the system, state of

charge of all the PEVs, and charging/discharging power are shown in Fig. 2.7. The PEVs with low initial SOC, PEV#1, #2, and #3, initially charge from the grid at a lower charging rate since the electricity price is high, but voltage constraints are satisfied at the buses where these are connected. Later, when the price of electricity is relaxed, all the PEVs charge from the grid at the maximum charging rate except PEV#3, which is connected to Node #18. As shown in Fig. 2.7, the re-distribution of the PEV charging load during the entire connection period results in shifting the PEV load from peak price to off-peak price period. The dash '-' lines represent the envelope of maximum and minimum limits for charging rate and PEV battery SOC in Fig. 2.7 (a) and (c), respectively. The voltage at Node #18 is at a lower tolerance limit, as shown in Fig. 2.6. Thus, PEV#3 is still unable to exploit the TOU tariff structure to the fullest possibility.

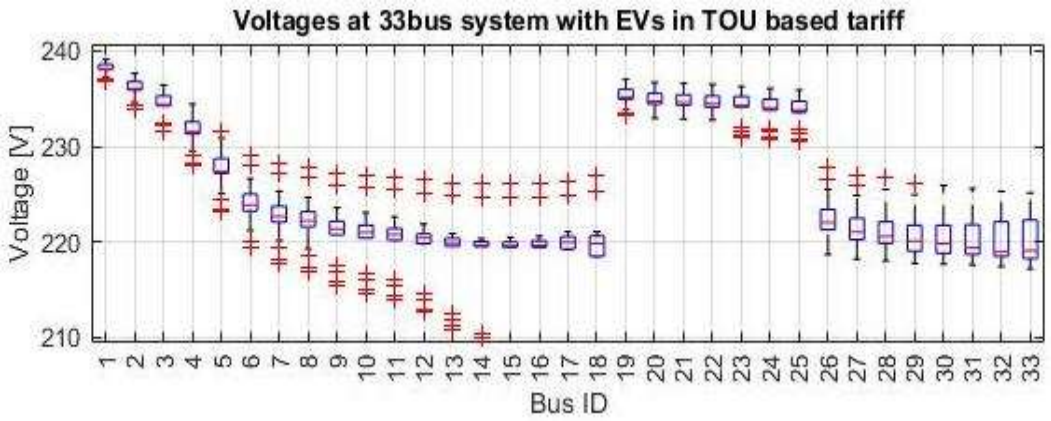

Fig. 2.6 Voltage distribution in the system with PEVs in TOU-based tariff structure.

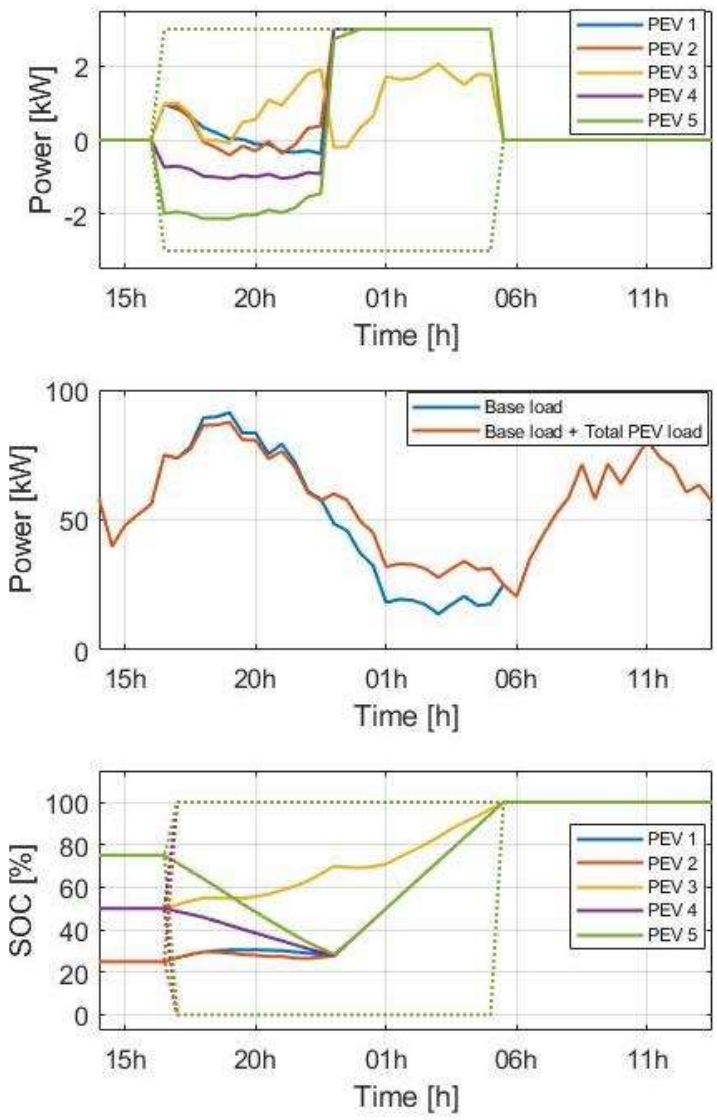

Fig. 2.7 (a) Charging/Discharging rate of PEVs, (b) Active power load in the system without and with PEVs, (c) SOC of the PEVs battery in TOU-based tariff structure.

The comparison of the charging costs of PEVs in two tariff scenarios is presented in Fig. 2.8. The charging cost has been optimized using equation (2.12), where battery degradation cost is also included. It is observed from Fig. 2.8 that charging cost reduces considerably for PEV#1, #2, #4 and #5 if the proposed charging scheme is adopted in the TOU-based tariff structure. However, the TOU-based tariff results in an increase in the

charging cost of PEV#3 as it is unable to fully exploit the benefit of this tariff due to low voltage at its point of connection.

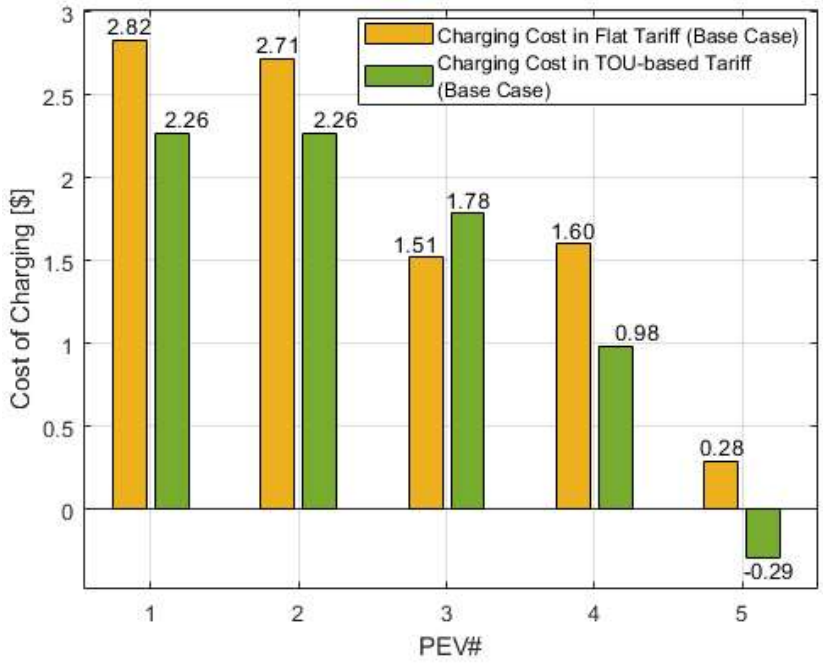

Fig. 2.8 Cost of charging of PEVs in the system without re-configuration.

2.6.2 Network re-configuration

The bus voltages are improved when the test system is re-configured, as shown in Fig. 2.9. The minimum system voltage without PEVs under network re-configuration is 222.07 V at Bus#32. This improved voltage profile provides extra flexibility to the PEV charging/discharging schedule.

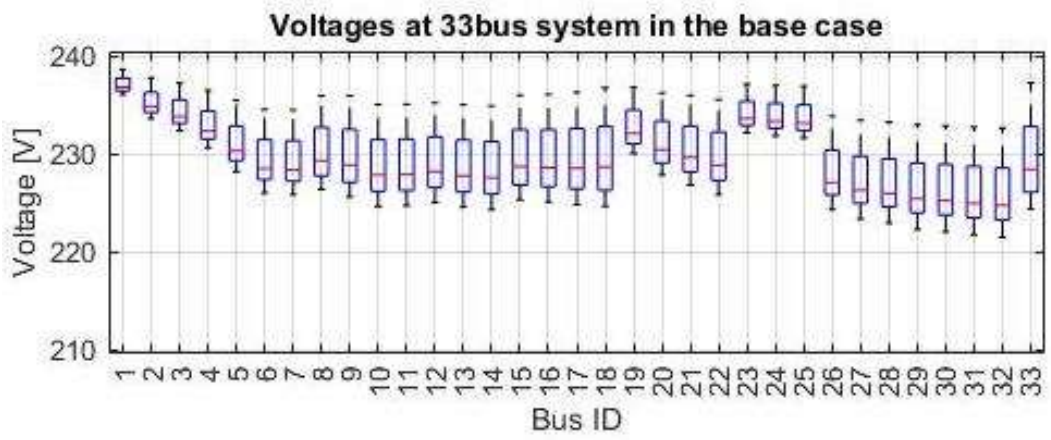

Fig. 2.9 Voltage distribution in the system without PEVs in the re-configured network.

Voltage distribution in the re-configured system is shown in Fig. 2.10 after the connection of five PEVs. The charging/discharging rate, system load, and SOC of the PEVs are shown in Fig. 2.11. As discussed, the reduction in charging cost also depends on the location of the PEVs. In the absence of network re-configuration, the connection of PEV#3 at Node#18 results in a voltage magnitude of 207V at this node, which corresponds to the minimum permissible voltage limit. By re-configuring, the voltages at each bus are improved.

The cost of charging PEVs in the re-configured network in both tariff scenarios is presented in Fig. 2.12. The charging cost has been minimized using equation (2.12), where battery degradation cost is also included. It is observed from Fig. 2.12 that the charging cost for PEV#3 reduces from \$1.78 to \$1.00. A 43.82% reduction in the charging cost of PEV#3 is achieved by re-configuring the network. Thus, PEV#3, which was unable to exploit the benefit of TOU-based tariff, is considerably benefited under network re-configuration. The overall charging cost is reduced by 11.15% for the five PEVs if the network is re-configured.

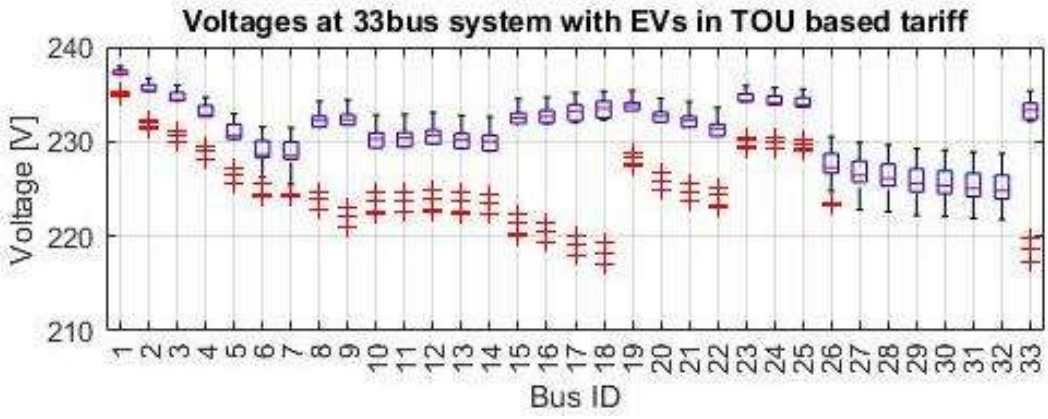

Fig. 2.10 Voltage distribution in the system with PEVs in TOU-based tariff structure in the re-configured network.

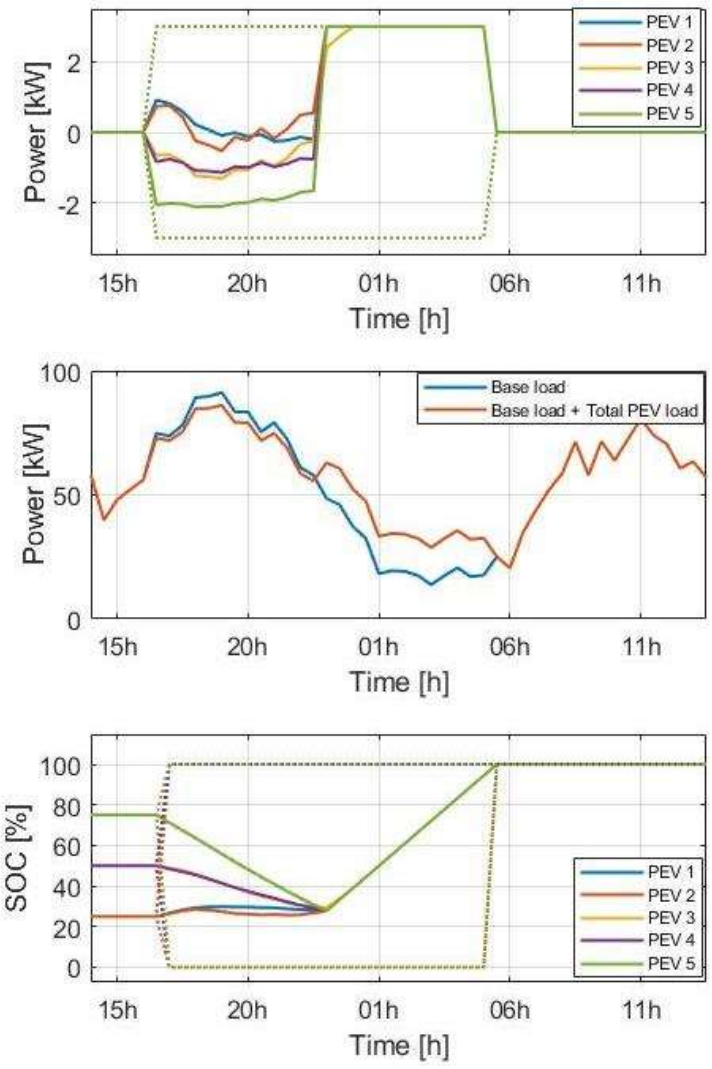

Fig. 2.11 (a) Charging/Discharging rate of PEVs, (b) Active power load in the system without and with PEVs, (c) SOC of the PEVs battery in TOU-based tariff structure in the re-configured network.

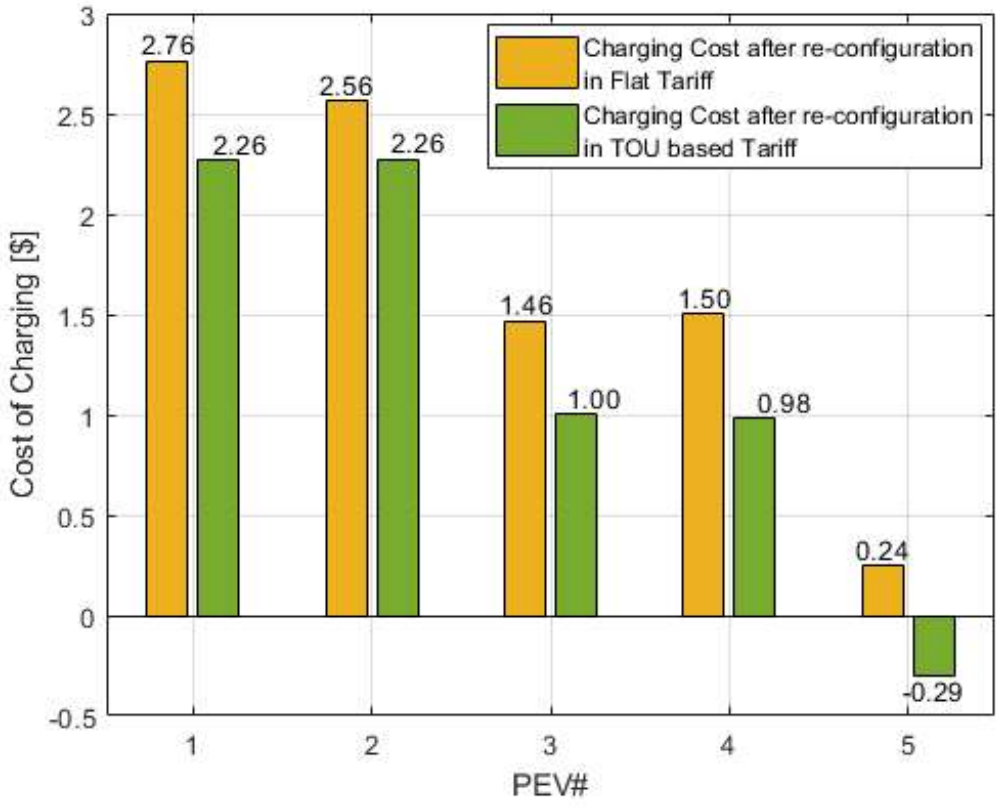

Fig. 2.12 Cost of charging of PEVs in re-configured Network.

2.6.3 Optimal charging of PEVs in the presence of Conservation Voltage Reduction (CVR)

The present work has considered the ZIP model for all residential loads. Table 2.2 shows the ZIP model coefficients for the class of residential equipments.

Table 2.2 ZIP model coefficients for residential customers [93].

Class	Z_p	I_p	P_p
Residential Customers	0.85	-1.12	1.27

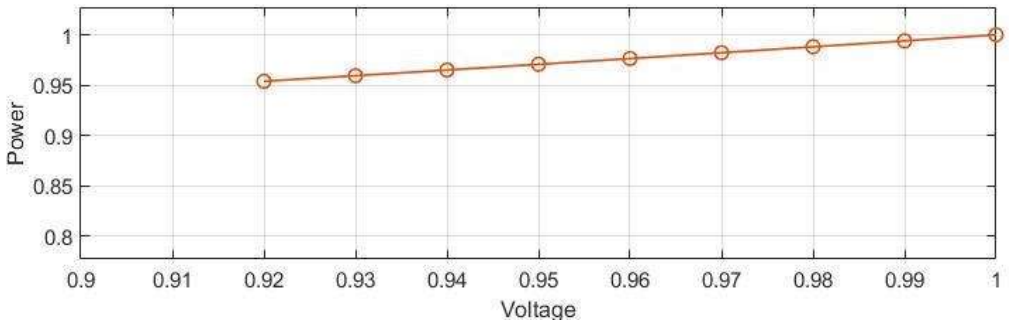

Fig. 2.13 Power requirement by the loads while performing voltage reduction.

Fig. 2.13 shows the power consumed by the loads modelled using ZIP coefficients for 0-0.08 p.u. of voltage reduction, and correspondingly the associated cost in TOU-based tariff is shown in Fig. 2.14. The cost of energy consumed by the loads after deployment of CVR (with 8% voltage reduction) is \$216.3 compared to \$226.7 in the absence of CVR.

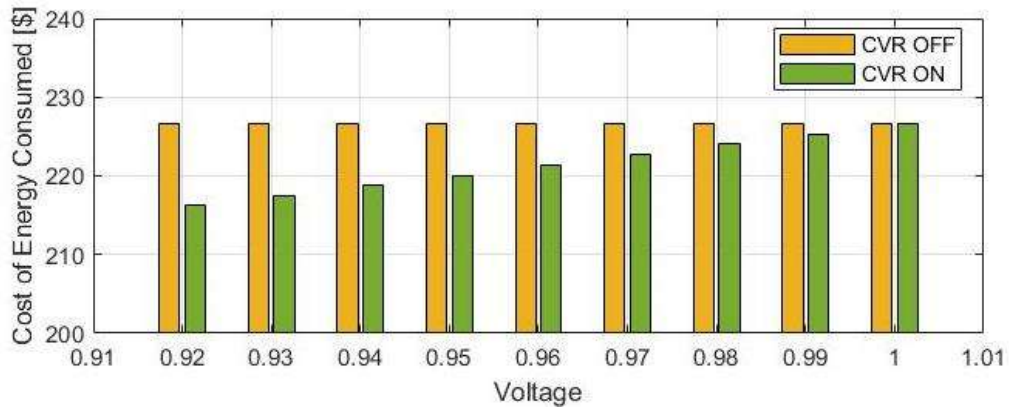

Fig. 2.14 Cost of energy consumed by loads before and after deployment of CVR.

The comparison between the charging cost of PEVs and minimum node voltage in the system in the case of optimal charging in TOU-based tariff without re-configuration and CVR, optimal charging of PEVs in the re-configured network under the TOU-based tariff, and optimal charging of PEVs in the re-configured network after deployment of CVR under the TOU-based tariff are shown in Table 2.3. The charging cost shown in Table 2.3

includes battery degradation cost as well. The optimal scheduling of PEVs shifts the charging load to off-peak load hours that result in the improvement of the system voltages. Network re-configuration alters the system parameters. Consequently, the PEVs are exposed to the modified system operating conditions. As observed from Table 2.3, network re-configuration in the absence of CVR substantially improves the node voltages and results in the highest reduction in charging costs of PEVs compared to other cases. The introduction of CVR (with 8% voltage reduction) in the re-configured network also leads to a considerable reduction in the charging cost of PEVs though it is less than the cost corresponding to the case of re-configuration without CVR deployment.

Table 2.3 Comparison of charging cost of PEVs and minimum system voltage in three different simulated cases.

Items	Optimal Charging of PEVs (TOU-based tariff)	Optimal Charging of PEVs with Network Re-configuration (TOU-based tariff)	Optimal Charging of PEVs with Network Re-configuration with CVR deployment (TOU-based tariff)
Tie-switches	33, 34, 35, 36, 37	7, 9, 14, 32, 37	7, 9, 14, 32, 37
Min. System Voltage without PEVs	209.61 V (18)	222.07 V (32)	211.6 V (32)
Min. System Voltage with PEVs in TOU-based Tariff	207 V (18)	216.58 V (18)	207 V (18)
Charging Cost with PEVs in TOU-based tariff	$6.99	$6.21	$6.84
Reduction in Charging Cost from Dumb Charging	50.24%	55.79%	51.31%

Fig. 2.15 presents the optimal charging cost, including the battery degradation cost of PEVs under the TOU-based tariff for the following three cases:

1. Original network with no re-configuration and CVR deployment.
2. Re-configured network without CVR.
3. Re-configured network with CVR.

As shown in Table 2.3 and Fig. 2.15, the overall charging cost of the PEVs after deployment of CVR in the re-configured network is $6.84 compared to $6.21 in the absence of CVR deployment in the re-configured network. This increase is acceptable since all the PEV and system constraints are still satisfied with a $10.4 reduction in the cost of energy consumed by the loads.

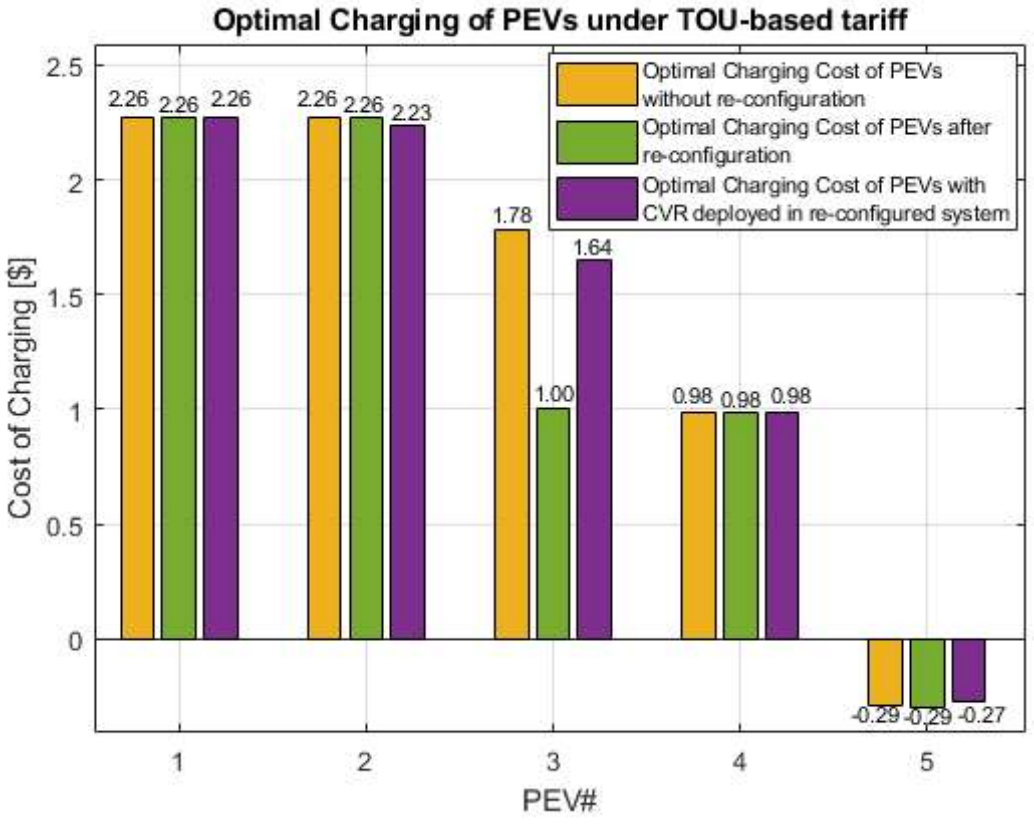

Fig. 2.15 Cost of charging of PEVs in three different simulated cases.

The profit of EV owner is over-rated if battery degradation cost is discarded. Fig. 2.16 shows the cost of charging all the PEVs during the entire connection period under a TOU-based tariff with network re-configuration but no CVR when battery degradation cost is discarded. The overall charging cost of the schedule is calculated to be $5.12 if the battery degradation cost is ignored, in contrast to $6.21, as shown in Table 2.3, when the battery degradation cost is considered. It indicates that ignorance of battery degradation cost yields under-estimation of PEV charging cost.

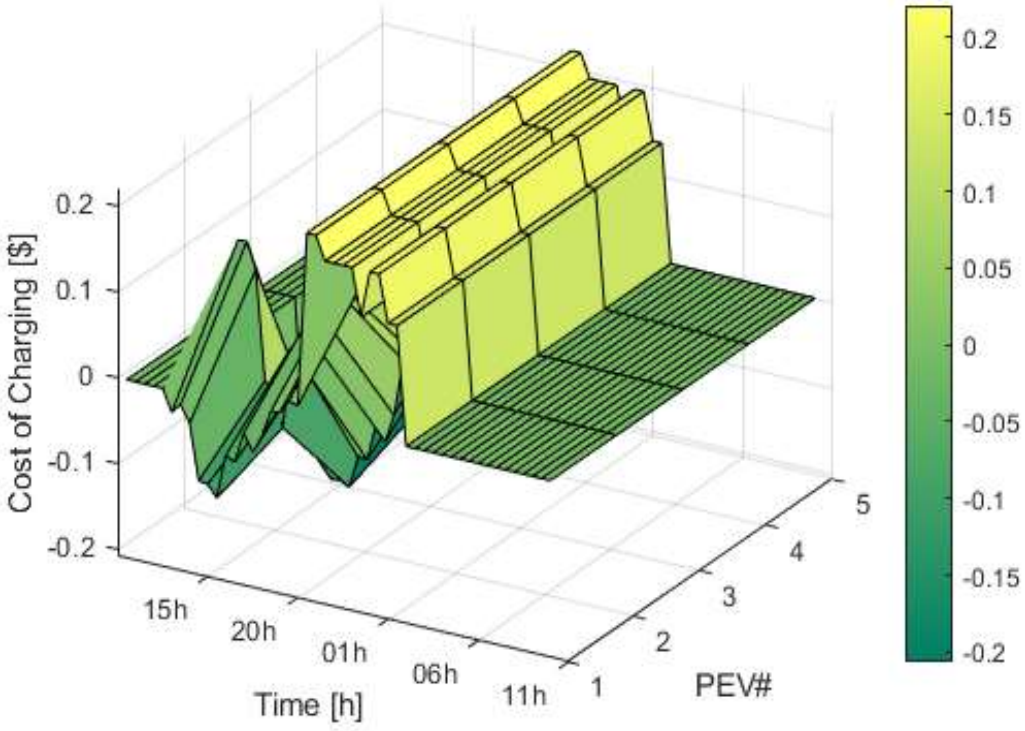

Fig. 2.16 Cost of charging of PEVs discarding battery degradation cost under TOU-based tariff with network re-configuration.

Further, optimistic results from an EV owner's perspective can be obtained when the initial SOC of the battery is near its capacity. For such a case, less amount of energy is required to fully charge the PEV battery. The optimal charging cost with an initial SOC of 100%, 75%, 50%, 75% and 100% for PEV#1, PEV#2, PEV#3, PEV#4 and PEV#5, respectively, is shown in Fig. 2.17. It is observed from the figure that the total charging

cost for this case is -$0.4768. It shows that if PEVs have sufficiently high initial SOC, they can earn a substantial benefit due to their discharging during peak price hours.

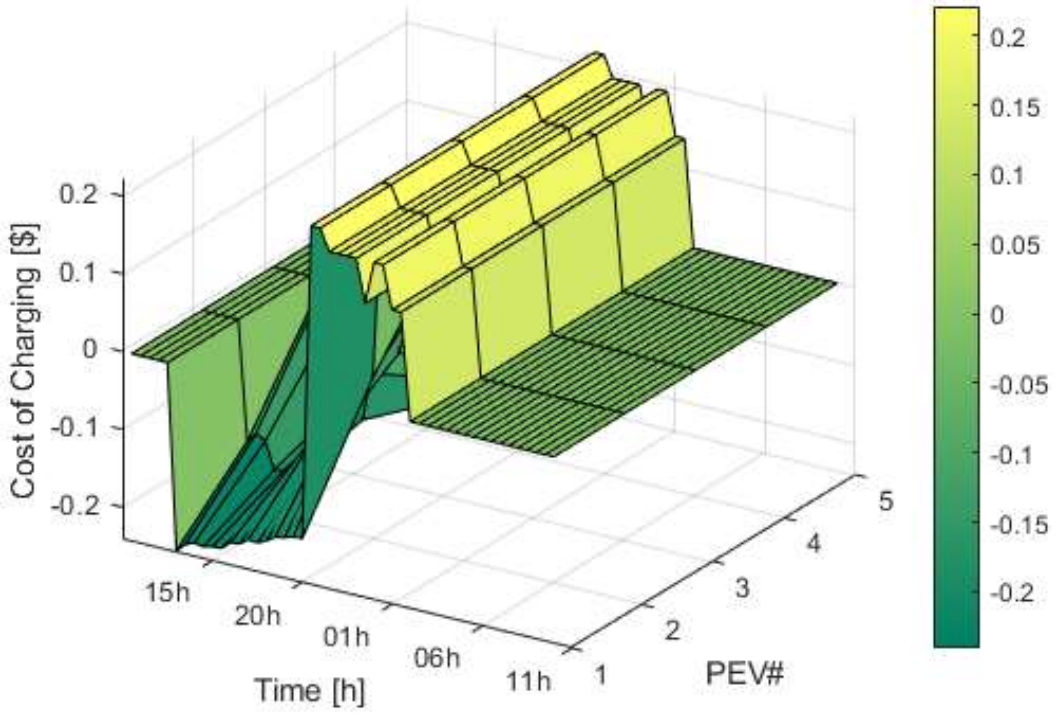

Fig. 2.17 Cost of charging of PEVs with initial SOC near the battery capacity under TOU-based tariff with network re-configuration.

2.7 RESULTS AND DISCUSSION

From the case study presented in Section 2.6., the following observations and inferences are drawn:

1. It is observed from Fig. 2.5 and Fig. 2.6 that the voltage profile resulting from the PEVs load could have deteriorated. However, shifting PEV charging from peak hours to off-peak hours and their discharge during peak hours in the TOU-based tariff is able to restrain voltage deterioration.

2. PEV#3 connected at Node#18 cannot exploit the TOU tariff as the voltage at Node#18 is at a lower tolerance limit. However, it is observed from Fig. 2.6 that the

voltage at Node#18 also gets enhanced as a result of the introduction of the TOU-based tariff. This is due to the shifting of charging of other PEVs from peak hours to off-peak hours, resulting in re-distribution of power flow among branches relieving heavily loaded branches.

3. It is observed from Fig. 2.8 that the charging cost of PEV#3 increases slightly after the introduction of the TOU-based tariff. This is due to the fact that Node#18 is heavily loaded, and every PEV needs to be fully charged by the indicated departure time. As PEV#3 charges during peak hours instead of discharging, as shown in Fig. 2.7 (c), it increases the charging cost.

4. The cost of PEV#5 charging becomes negative after introducing the TOU-based tariff, as shown in Fig. 2.8. This indicates that the EV owner earns profit from the entire charging schedule.

5. Re-configuration of the network flattens the voltage profile of the system, as shown in Fig. 2.9. It is due to the re-distribution of power flow among branches by shifting of power flow from heavily loaded branches to lightly loaded branches.

6. The comparison of Fig. 2.6 and Fig. 2.10 shows that the voltage profile is improved and flattens after re-configuration.

7. The voltage at Node#18 no more remains at the lower tolerance limit once the network is re-configured. Hence, PEV#3 is also able to exploit the TOU-based tariff by shifting its charging from peak hours to off-peak hours. It is observed from Fig. 2.8 and Fig. 2.12 that exploitation of the TOU-based tariff by PEV#3 results in a reduction in its charging cost from $1.78 (base case) to $1.00, which amounts to a 43.82% charging cost reduction.

8. The comparison of Fig. 2.8 and Fig. 2.12 shows that re-configuration results in the reduction of the charging cost of all the PEVs, even in the absence of the TOU-based tariff. The introduction of the TOU-based tariff further reduces the charging cost of all the PEVs. In the case of the TOU-based tariff structure, network re-configuration is unable to reduce further the charging cost of PEV#1, PEV#2, PEV#4 and PEV#5. However, a significant reduction in the charging cost of PEV#3 (from $1.78 to $1.00) leads to a considerable reduction in total charging cost. Therefore, EV charging under network re-configuration is more beneficial.

9. With re-configuration under the TOU-based tariff, PEV#5 charging cost still remains negative, indicating the profit earning of the EV owner from the entire charging schedule.

10. It is observed from Table 2.3 and Fig. 2.15 that introduction of CVR in the re-configured network under the TOU-based tariff structure is also beneficial in reducing the total charging cost of PEVs. However, charging cost reduction after deployment of CVR is less compared to the case without CVR. After the deployment of CVR, the cost reduction is achieved from the reduction in energy consumed by the constant impedance loads, which leads to a reduction in the total cost of energy consumption. Hence, PEV charging in the TOU-based tariff structure under network re-configuration and CVR deployment is beneficial for consumers.

11. Non-consideration of battery degradation cost leads to under-estimation of PEV charging cost. It is observed from Fig. 2.16 that the total charging cost of PEVs under the TOU-based tariff structure with network re-configuration under CVR deployment is calculated to be $5.12 while discarding the battery degradation cost as compared to $6.21 while battery degradation cost is considered.

12. It is observed from Fig. 2.17 that overall charging cost is reduced if PEVs have high initial SOC as the time required to fully charge the PEVs is less in such a case.

2.8 SUMMARY

In this work, an optimal V2G/G2V control scheme was proposed wherein PEV charging cost was reduced, satisfying the system constraints. Under certain assumptions, a linear programming technique was employed for PEVs load scheduling over the available charging period. In the V2G scheme, PEVs with available energy in the battery assist the system voltage. The proposed PEV charging scheme suggests re-configuration of the distribution network to redirect the power flow from heavily loaded to lightly loaded branches. This results in the flattening of the load profile and provides more freedom for PEV owners to charge during off-peak hours for maximizing profit. Network re-configuration was supported further with CVR to reduce energy consumed by constant impedance loads. Though this resulted in a slight increase in PEV charging cost, overall system operating cost was reduced owing to a higher reduction in energy consumed by constant impedance loads. The proposed scheme was evaluated on a modified IEEE 33-bus radial distribution system, and multiple cases were simulated. The obtained results confirmed the efficiency of the proposed scheme, wherein the charging cost of all the PEVs was reduced. Every PEV was charged to the desired SOC before the indicated departure time to ensure customer satisfaction. It is confirmed that in the TOU-based tariff structure, the PEV owner with sufficient initial SOC could obtain more profit by injecting power into the system during peak price hours in the re-configured network environment.